High Resolution Surface Imaging using a Carbon Nanotube Array with Pointed Height Distribution

Roy Mahapatra, D., Anand, S.V., Sinha, N., and Melnik, R.V.N.

Proc. 12th Annual NSTI Nanotech Conference, Nanotech Conference & Expo 2009, Technical Proceedings - Nanotechnology 2009, Eds. Laudon, M. and Romanowicz, B., Houston, Texas, May 3-7, 2009, USA, CRC Press, Vol. 1, 310-313,

ISBN: 978-1-4398-1786-5, 2009.

High Resolution Surface Imaging Using a Carbon Nanotube Array with Pointed Height distribution

D. Roy Mahapatra*, S.V. Anand*, N. Sinha** and R.V.N. Melnik***

*Department of Aerospace Engineering, Indian Institute of Science, Bangalore 560012, India
**Department of Mechanical Engineering, Massachusetts Institute of Technology, Cambridge, MA 02139, USA
***M^{2}NeT Lab, Wilfrid Laurier University, Waterloo, ON N2L3C5, Canada

ABSTRACT

In this paper we discuss a new technique to image the surfaces of metallic substrates using field emission from a pointed array of carbon nanotubes (CNTs). We consider a pointed height distribution of the CNT array under a diode configuration with two side gates maintained at a negative potential to obtain a highly intense beam of electrons localized at the center of the array. The CNT array on a metallic substrate is considered as the cathode and the test substrate as the anode. Scanning the test substrate with the cathode reveals that the field emission current is highly sensitive to the surface features with nanometer resolution. Surface features of semi-circular, triangular and rectangular geometries (projections and grooves) are considered for simulation. This surface scanning/mapping technique can be applied for surface roughness measurements with nanoscale accuracy, micro/nano damage detection, high precision displacement sensors, vibrometers and accelerometers, among other applications.

Keywords: carbon nanotube, field emission, surface imaging, pointed height distribution, array, sensor.

1 INTRODUCTION

Field emission from Carbon Nanotubes (CNTs) was first reported in 1995 by three research groups [1]-[3]. With significant research attention, CNTs are currently ranked among the best field emitters. CNTs grown on substrates are used as electron sources in field emission applications. One such application of significant interest is the use of CNT based field emission in imaging devices like electron microscopes [4]-[6]. However, fluctuation of field emission current from CNTs poses certain difficulties in their use in imaging probes and X-ray devices. This problem arises due to deformation of the CNTs due to electrodynamic force field and electron-phonon interaction. It is of great importance to have precise control of emitted electron beams right near the CNT tips.

Field emission from CNTs is difficult to characterize using simple formulae or data fitting, which is due to (1) electron-phonon interaction; (2) electromechanical force field leading to stretching of CNTs; and (3) ballistic transport induced thermal spikes, coupled with high dynamic stress, resulting in degradation of emission performance at the device scale. Fairly detailed physics-based models of CNTs considering the aspects (1) and (2) above have already been developed by the authors [7]-[11]. A new array configuration with stacked array of CNTs with pointed height distribution of the CNTs was analyzed by the authors [12]- [13] and it was shown that the current density distribution is greatly localized at the middle of the array, the scatter due to electrodynamic force field was minimized and the temperature transients were much smaller compared to those in an array with random height distribution.

In the present paper, the proposed pointed array configuration of the CNTs on a metallic cathode substrate is used to image the surfaces of metallic substrates. This is done my making the test substrate as the anode and scanning the surface by moving the cathode over it in controlled paths (for e.g. a Raster scan). Since, the new configuration with additional side gates provides a highly intense beam of electrons localized at the center of the array (diameter of the electron beam is comparable to the diameter of a CNT), surface features of the order of a few nano meters are imaged with high degree of accuracy. We perform simulations on assumed surface features of semi-circular, triangular and rectangular geometries (projections and grooves) and prove that the discussed method is highly sensitive and equally accurate in reproducing minute surface features.

2 MODELING APPROACH

Let N_T be the total number of carbon atoms (in CNTs and in cluster form) in a representative volume element ($V_{\text{cell}} = \Delta A d$), where ΔA is the cell surface interfacing the anode and d is distance between the inner surfaces of cathode substrate and the anode. Let N be the number of CNTs in the cell, and N_{CNT} be the total number of carbon atoms present in the CNTs. We assume that during field emission some CNTs are decomposed and form clusters. Such degradation and fragmentation of CNTs can be treated as the reverse process of CVD or a similar growth process used for producing the CNTs on a substrate. Hence,

$$N_T = N N_{CNT} + N_{\text{cluster}} \,, \tag{1}$$

where N_{cluster} is the total number of carbon atoms in the clusters in a cell at time t and is given by

$$N_{\text{cluster}} = V_{\text{cell}} \int_0^t dn_1(t) \ , \tag{2}$$

where n_1 is the concentration of carbon clusters in the cell. By combining Eqs. (1) and (2), one has

$$N = \frac{1}{N_{CNT}} \left[N_T - V_{\text{cell}} \int_0^t dn_1(t) \right] . \tag{3}$$

The number of carbon atoms in a CNT is proportional to its length. Let the length of a CNT be a function of time, denoted as $L(t)$. Therefore, one can write

$$N_{CNT} = N_{\text{ring}} L(t) \ , \tag{4}$$

where N_{ring} is the number of carbon atoms per unit length of a CNT and can be determined from the geometry of the hexagonal arrangement of carbon atoms in the CNT. By combining Eqs. (3) and (4), one can write

$$N = \frac{1}{N_{\text{ring}} L(t)} \left[N_T - V_{\text{cell}} \int_0^t dn_1(t) \right] . \tag{5}$$

In order to determine $n_1(t)$ phenomenologically, we employ a nucleation coupled model developed by us previously [7]. Based on the model, the rate of degradation of CNTs (v_{burn}) is defined as

$$v_{\text{burn}} = V_{\text{cell}} \frac{dn_1(t)}{dt} \left[\frac{s(s-a_1)(s-a_2)(s-a_3)}{n^2 a_1^2 + m^2 a_2^2 + nm(a_1^2 + a_2^2 - a_3^2)} \right]^{1/2} , \tag{6}$$

where a_1, a_2, a_3 are lattice constants, $s = \frac{1}{2}(a_1 + a_2 + a_3)$, n and m are integers ($n \geq |m| \geq 0$). The pair (n, m) defines the chirality of the CNT. Therefore, at a given time, the length of a CNT can be expressed as $h(t) = h_0 - v_{\text{burn}} t$, where h_0 is the initial average height of the CNTs and d is the distance between the cathode substrate and the anode.

In the absence of electronic transport within a CNT and field emission from its tip, the background electric field is simply $E_0 = -V_0/d$, where $V_0 = V_d - V_s$ is the applied bias voltage, V_s is the constant source potential on the substrate side, V_d is the drain potential on the anode side and d, as before, is the clearance between the electrodes. The total electrostatic energy consists of a linear drop due to the uniform background electric field and the potential energy due to the charges on the CNTs. Therefore, the total electrostatic energy can be expressed as

$$\mathcal{V}(x, z) = -eV_s - e(V_d - V_s)\frac{z}{d} + \sum_j G(i, j)(\hat{n}_j - n) \ , \tag{7}$$

where e is the positive electronic charge, $G(i, j)$ is the Green's function [14] with i indicating the ring position and $\hat{n}_j$ describing the electron density at node position j on the ring. In the present case, while computing the Green's function, we also consider the nodal charges of the neighboring CNTs. This essentially introduces non-local contributions due to the CNT distribution in the film. We compute the total electric field $\mathbf{E}(z) = -\nabla\mathcal{V}(z)/e$, which is expressed as

$$E_z = -\frac{1}{e}\frac{d\mathcal{V}(z)}{dz} \ . \tag{8}$$

The current density (J) due to field emission is obtained by using the Fowler-Nordheim (FN) equation [15]

$$J = \frac{BE_z^2}{\Phi} \exp\left[-\frac{C\Phi^{3/2}}{E_z} \right] , \tag{9}$$

where Φ is the work function of the CNT, and B and C are constants. Computation is performed at every time step, followed by update of the geometry of the CNTs. As a result, the charge distribution among the CNTs also changes and such a change affects Eq. (7). The field emission current (I_{cell}) from the anode surface corresponding to an elemental volume V_{cell} of the film is then obtained as

$$I_{\text{cell}} = A_{\text{cell}} \sum_{j=1}^{N} J_j \ , \tag{10}$$

where A_{cell} is the anode surface area and N is the number of CNTs in the volume element. The total current is obtained by summing the cell-wise current (I_{cell}). This formulation takes into account the effect of CNT tip orientations, and one can perform statistical analysis of the device current for randomly distributed and randomly oriented CNTs.

3 SIMULATION METHODOLOGY

In the simulation and analysis, the distance between the cathode substrate and flat anode surface was taken as 34.6 μm. Fig. 1 shows the schematic representation

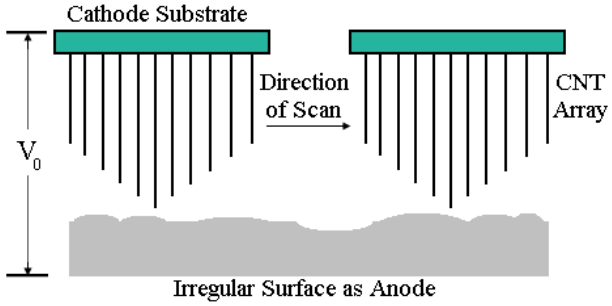

Figure 1: A schematic diagram of the pointed CNT array grown on a metallic cathode substrate scanning a substrate, whose surface has to be imaged.

NSTI-Nanotech 2009, www.nsti.org, ISBN 978-1-4398-1782-7 Vol. 1, 2009

of the pointed CNT array scanning the test surface. Surface features of various geometries like semi-circular, triangular and rectangular are assumed for simulation. Each of the surface feature is considered as a projection and groove on the flat surface of the anode. The maximum height of these features is limited to 300 nm. Due to computational limitations each feature is divided into only nine points where the scan is performed. Increasing the number of scan points will significantly improve the resulting current profile. The height of CNTs in the array varies from 6 μm at the edges to 12 μm at the centre of the array. The constants B and C in Eq. (9) were taken as $(1.4 \times 10^{-6}) \times \exp((9.8929) \times \Phi^{-1/2})$ and 6.5×10^{7}, respectively [16].

4 RESULTS AND DISCUSSIONS

Fig. 2 shows the spatial distribution of emission current density in the pointed array as compared to other array configurations like uniform, random and V-shape. It is clear that the emission is stable and it is focused towards the middle of the array. This is a very important

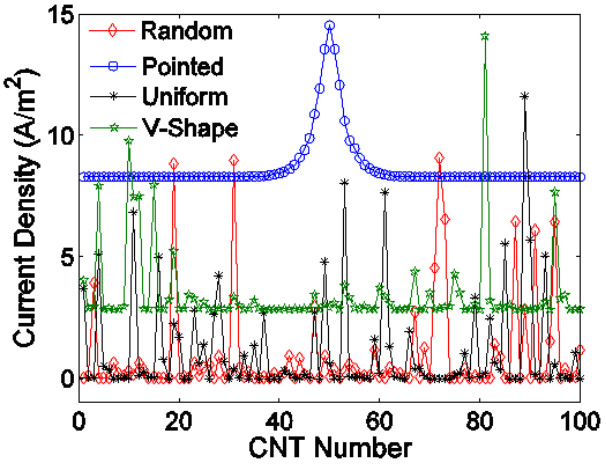

Figure 2: Current density distribution at the tips of 100 carbon nanotubes considered in the array with various height distributions. The current density distribution for the pointed array is focused at the centre of the array with a beam diameter comparable to the diameter of a single CNT.

phenomenon observed only in the pointed array configuration, which enables it to be used for surface scanning.

Figs. 3-8 show the schematic diagrams of the various surface features considered for simulation and the respective field emission current profiles obtained after the scans. Each feature is divided into nine equally spaced points (a-i), where the scans are performed. It is evident from Figs. 3-8 that the topography of the minute (300 nm) features is captured very effectively with spatial resolutions as small as 10 nm.

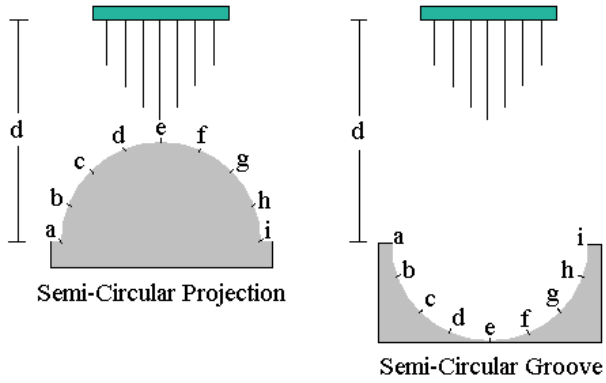

Figure 3: A semi-circular projection and groove of 300 nm radius on the surface of a substrate considered for simulation. The distance between the cathode and the flat surface of the anode (d) is 34.6 μm. The projection and the groove are scanned at 9 different points (a-i).

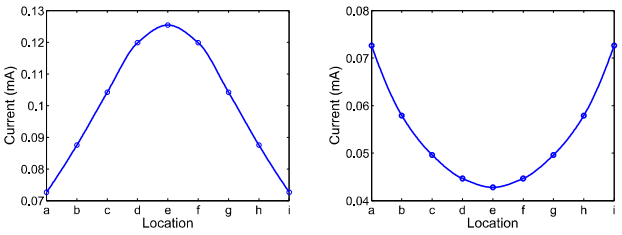

Figure 4: Field emission current profile obtained by scanning (a) semi-circular projection on the surface of the anode (b) semi-circular groove on the surface of the anode.

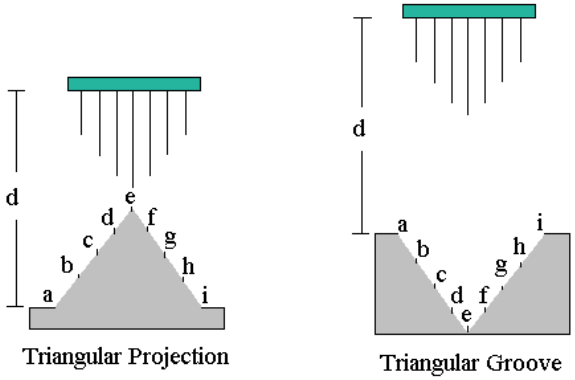

Figure 5: A triangular projection and groove of 300 nm height on the surface of a substrate considered for simulation. The distance between the cathode and the flat surface of the anode (d) is 34.6 μm. The projection and the groove are scanned at 9 different points (a-i).

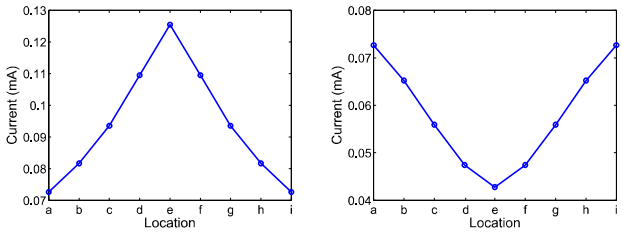

Figure 6: Field emission current profile obtained by scanning (a) triangular projection on the surface of the anode (b) triangular groove on the surface of the anode.

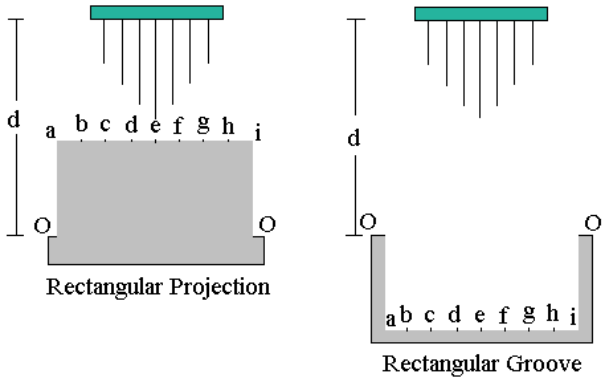

Figure 7: A rectangular projection and groove of 300 nm height on the surface of a substrate considered for simulation. The distance between the cathode and the flat surface of the anode (d) is 34.6 μm. The projection and the groove are scanned at 9 different points (a-i).

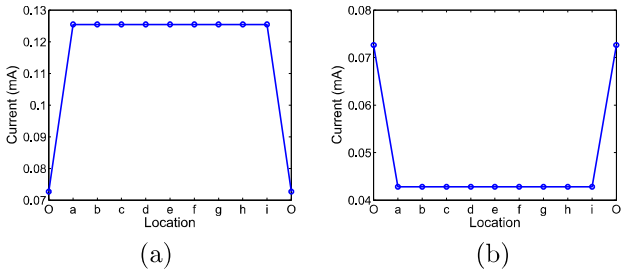

Figure 8: Field emission current profile obtained by scanning (a) rectangular projection on the surface of the anode (b) rectangular groove on the surface of the anode.

5 CONCLUSION

In this paper a new technique to image the surfaces of metallic substrates using field emission from a pointed array of carbon nanotubes has been proposed. A pointed height distribution of the carbon nanotube array under a diode configuration is considered to obtain a highly intense beam of electrons localized at the centre of the array. Simulations are performed on various assumed surface features of standard geometries and the resulting field emission current profiles are plotted. The proposed method of scanning is very effective as it captures the topography of the surface features accurately with a resolution of almost 10 nm. This technique can be applied for surface roughness measurements with nanoscale accuracy, micro/nano damage detection, high precision displacement sensors, vibrometers and accelerometers, among other applications.

REFERENCES

[1] A. G. Rinzler, J. H. Hafner, P. Nikolaev, L. Lou, S. G. Kim, D. Tomanek, D. Colbert and R. E. Smalley, Science 269, 1550, 1995.

[2] W. A. de Heer, A. Chatelain and D. Ugrate, Science 270, 1179, 1995.

[3] L. A. Chernozatonskii, Y. V. Gulyaev, Z. Y. Kosakovskaya, N. I. Sinitsyn, G. V. Torgashov, Y. F. Zakharchenko, E. A. Fedorov and V. P. Valchuk, Chem. Phys. Lett. 233, 63, 1995.

[4] Q. H. Wang, A. A. Setlur, J. M. Lauerhaas, J. Y. Dai, E. W. Seelig, and R. P. H. Chang, Appl. Phys. Lett. 72, 2912, 1998.

[5] W. B. Choi *et al.*, Appl. Phys. Lett. 75, 3129, 1999.

[6] O. Lourie and H. D. Wagner, Appl. Phys. Lett. 73, 3527, 1998.

[7] N. Sinha, D. Roy Mahapatra, J.T.W. Yeow, R.V.N. Melnik and D. A. Jaffray, Proc. IEEE Int. Conf. Nanotech., 673, 2006.

[8] N. Sinha, D. Roy Mahapatra, J.T.W. Yeow, R.V.N. Melnik and D.A. Jaffray, J. Comp. Theor. Nanosci. 4, 535, 2007.

[9] N. Sinha, D. Roy Mahapatra, Y. Sun, J.T.W. Yeow, R.V.N. Melnik and D.A. Jaffray, Nanotechnology 19, 25710, 2008.

[10] N. Sinha, D. Roy Mahapatra, J.T.W. Yeow and R.V.N. Melnik, Proc. IEEE Int. Conf. Nanotech., 961, 2007.

[11] D. Roy Mahapatra, N. Sinha, J.T.W. Yeow and R.V.N. Melnik, Appl. Surf. Sci. 255, 1959-1966, 2008.

[12] D. Roy Mahapatra, S. V. Anand, N. Sinha and R.V.N. Melnik, Mol. Sim. (In press, to appear in March 2009).

[13] D. Roy Mahapatra, N. Sinha, S. V. Anand, R. Krishnan, N. V. Vikram, R.V.N. Melnik and J. T. W. Yeow, Proc. 11th NSTI Nanotech. Conf. 1, 55-58, 2008.

[14] A. Svizhenko, M.P. Anantram and T.R. Govindan, IEEE Trans. Nanotech. 4, 557, 2005.

[15] R.H. Fowler and L. Nordheim, Proc. Royal Soc. London A 119, 173, 1928.

[16] Z. P. Huang, Y. Tu, D. L. Carnahan and Z. F. Ren, Encyclopedia of Nanoscience and Nanotechnology (Ed. H.S. Nalwa) 3, 401-416, 2004.

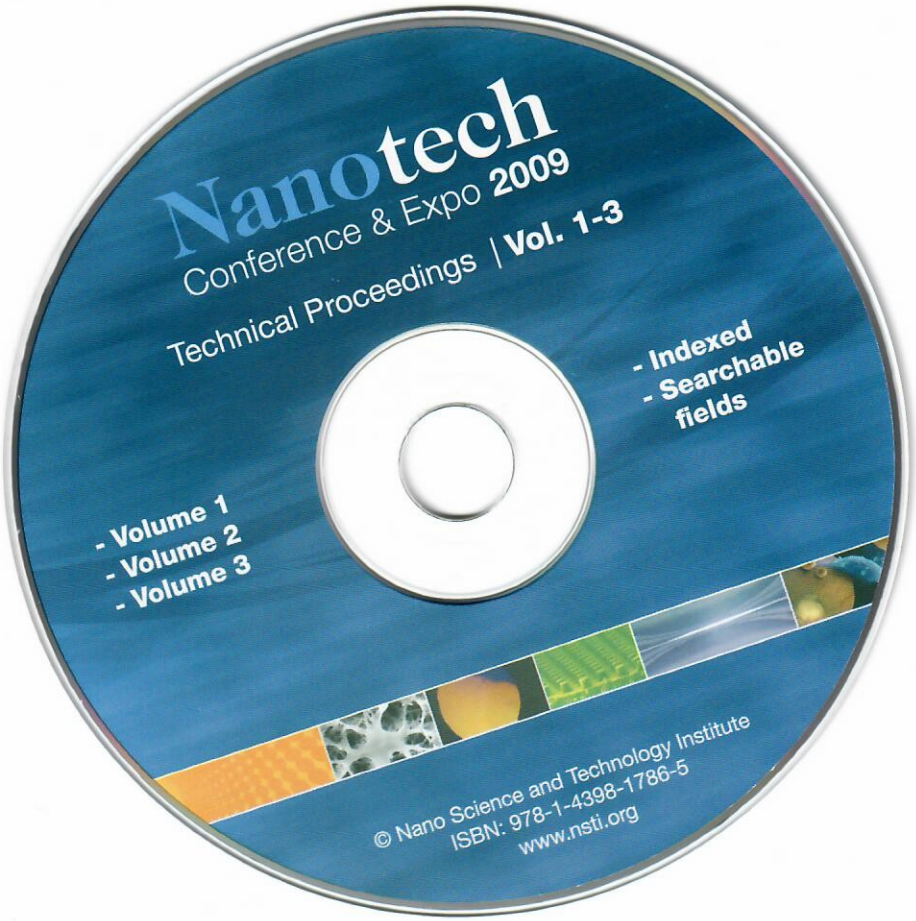
Nanotech
Conference & Expo 2009
Technical Proceedings | Vol. 1-3
- Volume 1
- Volume 2
- Volume 3
- Indexed
- Searchable fields
© Nano Science and Technology Institute
ISBN: 978-1-4398-1786-5
www.nsti.org

Nanotech
Conference & Expo 2009

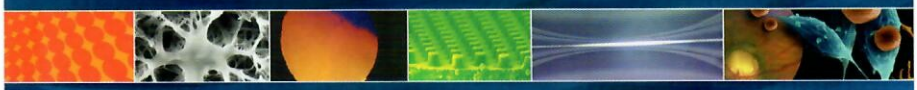

NSTI
Nano Science and Technology Institute

BioNano
Conference & Expo 2009

CRC Press
Taylor & Francis Group

Technical Proceedings | **Vol. 1-3**

Vol. 1: Fabrication, Particles, Characterization, MEMS, Electronics and Photonics

Vol. 2: Life Sciences, Medicine, Diagnostics, Bio Materials and Composites

Vol. 3: Biofuels, Renewable Energy, Coatings, Fluidics and Compact Modeling

Vol. 1
Nano Fabrication
Nanoparticles
Nanostructured Materials and Devices
Nanoscale Characterization
MEMS and NEMS
Wireless MEMS
Sensors and Systems
Nano Electronics and Photonics

Vol. 2
Cancer Nanotechnology
Drug Delivery
Nano Medicine
Biosensors and Diagnostics
Bio Nano Materials
Nano Bio Materials and Tissues
Environment, Water, Health,
Safety and Society
Polymer Nanotechnology
Nanocomposites

Vol. 3
Bio Energy and Bio Fuels
Energy, Storage, Fuel Cells, Hydrogen and Grid
Solar and PV Technologies
Coatings and Surfaces
Modeling and Simulation of Micro and Nano Systems
Nanotechnology Investment and Initiatives
Carbon Nano Structures
Micro and Nano Fluidics
Workshop on Compact Modeling

CRC Press
Taylor & Francis Group
an informa business
www.taylorandfrancisgroup.com

6000 Broken Sound Parkway, NW
Suite 300, Boca Raton, FL 33487
270 Madison Avenue
New York, NY 10016
2 Park Square, Milton Park
Abingdon, Oxon OX14 4RN, UK

ISBN: 978-1-4398-1786-5
90000
9 781439 817865